Arabian Journal of Chemistry (2020) **13**, 5430–5437

King Saud University

Arabian Journal of Chemistry

www.ksu.edu.sa
www.sciencedirect.com

ORIGINAL ARTICLE

Synthesis and characterization of $CoFe_2O_4@SiO_2$-polyethyleneimine magnetic nanoparticle and its application for ultrasonic-assisted removal of disulfine blue dye from aqueous solution

Maria Bektar, Hossein Ali Rasekh *, **Mohammad Jaafar Soltanianfard**

Department of Chemistry, Firoozabad Branch, Islamic Azad University, Firoozabad, Fars P.O. Box, 74715-117, Iran

Received 16 February 2020; accepted 22 March 2020
Available online 2 April 2020

KEYWORDS

$CoFe_2O_4@SiO_2$-polyethyleneimine;
Magnetic nanoparticles;
Removal;
Disulfine blue

Abstract In the present work, a simple synthesis approach was applied for the fabrication of $CoFe_2O_4@SiO_2$-polyethyleneimine magnetic nanoparticles as an effective sorbent for ultrasonic-assisted removal of disulfine blue dye from an aqueous solution. For identification and characterization of prepared sorbent, different analysis including Fourier transform infrared spectroscopy (FT-IR), Field emission scanning electron microscopy (FE-SEM), Vibrating sample magnetometer (VSM), Energy dispersive X-ray analysis (EDX) and Transmission electron microscopy (TEM) were applied. The effect of effective parameters on the removal of disulfine blue such as pH, sorbent mass, ultrasonic time and disulfine blue concentration were also assessed. The optimum values for investigated parameters were achieved to be as follows: pH of 5.0, sorbent mass of 0.015 g, ultrasonic time of 5.0 min and disulfine blue concentration of 10.0 mg L^{-1}. Different isotherm and kinetic models were used for the evaluation of isotherm and kinetic of adsorption. Results showed that the Langmuir isotherm model was better than other isotherm models as well as the second-order equation model was selected as a kinetic model. The maximum adsorption capacity of the proposed magnetic sorbent was achieved to be 110.0 mg g^{-1} which shows the applicability of proposed sorbent for removal of disulfine blue dye from aqueous solution.

1. Introduction

Water pollution is one of the most important challenges that the world faces. There are plenty of resources for pollution of water. Industrial and synthetic dyes are one of the main branches of these resources that not only can change the chemical and physical property of water but also can have adverse side effects (Homem et al., 2019; Tanhaei et al., 2019). These

---

* Corresponding author.
E-mail address: Hossein.ali_Rasekh@yahoo.com (H. Ali Rasekh).

Peer review under responsibility of King Saud University.

Production and hosting by Elsevier

https://doi.org/10.1016/j.arabjc.2020.03.022

dyes can cause chemical changes, consume dissolved oxygen and also generate the carcinogenic and genotoxic problem. So, they are harmful to both human health and the environment. Disulfine blue (DB) (Fig. 1.) is a synthetic dye that has been widely applied in different industries including coloring paper, temporary hair colorant, dyeing cottons, wools and so on (Bagheri et al., 2016b). In spite of its applications and advantages, it can cause some illnesses for humans. So, removing it from water resources is still a vital task. Different methods such as adsorption, membrane separation, flocculation–coagulation and aerobic or anaerobic treatment have been extensively used for removal of dyes from water (Bagheri et al., 2017b; Wang et al., 2020). Compare to other methods, the adsorption technique has been very much considered since it is a simple, easy, low cost and more applicable without the generation of hazardous intermediate products (Bagheri et al., 2017a; Li et al., 2020). Different sorbents have been applied for removal of dyes from wastewater which have main drawbacks in terms of low specific surface area as well as low binding capacity (Oussalah et al., 2019). In this regard, much attention has recently been paid to the use of nano-sized material due to their high surface area, presentation of highly porous structure and high adsorption capacity which can improve the dye adsorption efficiency (Bagheri and Ghaedi, 2020a, 2020b, 2020c; Bidgoli et al., 2019; Uogintė et al., 2019). One of the tedious and non-interesting stages in the adsorption process is the face separation difficulty and arrival of nano-scale based material to different ecosystem following usage. This difficulty and domination simply and efficiently can be overcome by using magnetic nano-scale material that can be separated by exposure to external magnetic fields (Arabi et al., 2020; Bagheri et al., 2019a; Bagheri et al., 2019b; Bagheri and Ghaedi, 2019; Khani et al., 2019). Iron-based magnetic nanostructures have distinguished properties which make them as a good candidate for using in different fields such as separation and removal of dyes from water resources (Yang et al., 2020a; Zangeneh et al., 2019). Nano-sized magnetic compounds have supreme physical and chemical properties due to their mesoscopic effect, small object effect, quantum size effect and surface effect (Arabi et al., 2016; Gholami et al., 2019a; Gholami et al., 2019b; Gholami et al., 2019c; Ostovan et al., 2018a; Ostovan et al., 2018b; Yang et al., 2020c). Recently, metal-oxide nanoparticles have been the subject of much interest because of their unusual optical, electronic and magnetic properties, which often differ from the bulk. Cobalt ferrite is an efficient magnetic compound that has distinguished properties in terms of mechanical hardness, high coercively, high cubic magneto crystalline anisotropy, high physical and chemical stability (Arabi et al., 2017; Guo et al., 2020; Maaz et al., 2007), and appropriate magnetization for separation using an external magnetic field (Ansari et al., 2019; Pastor-Belda et al., 2017). Cobalt (II) ions are more difficult to oxidize than the iron (II) and that consequently, cobalt ferrite nanoparticles are more stable over long times than Fe_3O_4 particles. Modification of magnetic nanoparticles is essential that is due to enhances their stability in different media as well as prevents the oxidation of them which can improve their performance. For this purpose, SiO_2 is a good choice that is due to exceptional properties of SiO_2 in terms of high chemical and physical properties and bio-compatibility that can modify magnetic nanoparticles surface completely and increase the physical and chemical stability of magnetic nanoparticles (Yang et al., 2019; Zhang et al., 2019). In addition, to increase the surface area of adsorbent, polyethyleneimine (PEI) is a good choice. PEI is a positive charge polyelectrolyte supplying a large number of nitrogen atoms corresponding to amino groups which contain primary, secondary, and tertiary amino groups in a ratio of approximately 1:2:1 (An and Gao, 2007; Yang et al., 2020b; Zhong and Jia, 2019; Zhou et al., 2016). Their combination with a number of polar groups (amino groups) in PEI affects their adsorption capability towards organic compounds. It will be a good method for modification of cobalt ferrite ($CoFe_2O_4$) nanoparticles with PEI and their association can be applied as an effective sorbent for separation and removal of DB from an aqueous solution. In this work, $CoFe_2O_4$@SiO_2-polyethyleneimine was synthesized as an effective sorbent for the removal of DB from an aqueous solution. It was characterized using different analysis such as FTIR, XRD, FE-SEM, VSM, EDX, and TEM. Also, the effect of influential parameters on DB removal including pH, sorbent mass, ultrasonic time and DB concentration was investigated and optimum levels were achieved. The results showed that prepared sorbent has good magnetic strong and adsorption capacity which make it as a good sorbent for removal of DB from an aqueous solution.

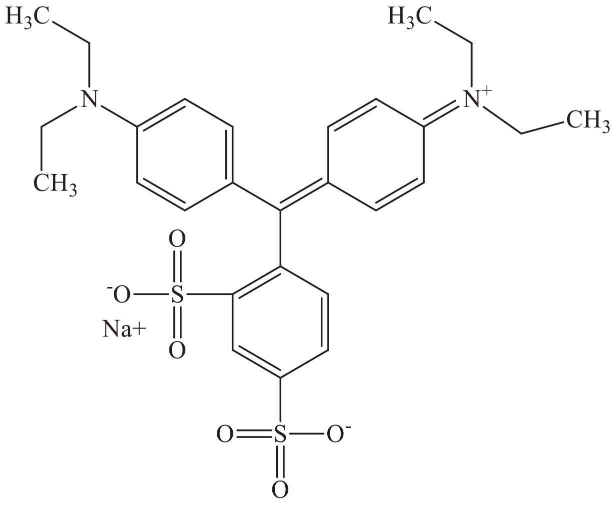

Fig. 1 Chemical structure of disulfine blue.

2. Experimental section

2.1. Chemicals, reagents and instrumental

All materials and reagents including DB dye, deionized water, ethanol, NaOH, HCl, NH_3 solution, tetraethylorthosilicate, methylbenzene, polyethyleneimine and (3-chloropropyl) trimethoxysilane were purchased from Merck Company. A pH-meter (Model 692, Metrohm AG, Herisau, Switzerland) was used for the pH measurements. Ultrasonic-assisted adsorption of DB was done in an ultrasonic bath (Tecno-GAZ SPA Ultra Sonic System, Parma, Italy) operated at a frequency of 40 kHz and 130 W of power with a useable volume of 3.0 L. The morphology analysis of obtained $CoFe_2O_4$@SiO_2-polyethyleneimine was carried out by scanning electron microscope (SEM, Hitachi S- 4160, Japan) under an acceleration voltage of 26 kV and transmission electron microscope (TEM, Hitachi H-800 at 200 kV, Japan), X-ray diffraction (XRD, Philips PW 1800 Holland, Netherland, 40 kV and 40 mA) and Fourier transformed infrared spectroscopy (FTIR, RX-IFTIR, Perkin Elmer). The concentration of the DB in the solution after equilibrium adsorption was measured by a double beam UV–Vis spectrophotometer (Shimadzu, Model UV 1601, Japan) at 637 nm.

2.2. Synthesis of $CoFe_2O_4$ nanoparticles

An aqueous solution of 0.2 M $CoCl_2 \cdot 6H_2O$ and 0.4 M $FeCl_3 \cdot 6H_2O$ were mixed under the ultrasonic irradiation for 30 min. Then, 0.2 M oleic acid solution was added to the mixture and subsequently, the 3 M solution of NaOH was added to adjust pH 8. Then, the mixture was heated under 80 °C for 1 h. In the following, the solution was cooled at room temperature, and the obtained precipitation was separated using an external magnetic as well as washed several times by deionized water and ethanol and dried at 60 °C.

2.3. Preparation of $CoFe_2O_4@SiO_2$

Coating of $CoFe_2O_4$ nanoparticles with a layer of silica was attained through the Stöber method which is based on the hydrolysis of tetraethylorthosilicate (TEOS) in the presence of NH_3 to obtain $CoFe_2O_4@SiO_2$ composite (Stöber et al., 1968). In this regard, 0.5 g of $CoFe_2O_4@SiO_2$ was reacted with 0.5 mL of (3-chloropropyl) trimethoxysilane in the presence of 100 mL methylbenzene. Then, the mixture was stirred at 110 °C for 12 h to obtain $CoFe_2O_4@SiO_2$-Cl. Then, the obtained $CoFe_2O_4@SiO_2$-Cl was reacted with 25 mL of an aqueous solution of polyethyleneimine at 90 °C for 6 h. Finally, $CoFe_2O_4$@PEI particle was washed with deionized water and ethanol several times and finally dried at 60 °C for 12 h.

2.4. Ultrasound-assisted adsorption method

Ultrasound-assisted experiments were conducted to investigate the effect of different factors on the removal of DB. The batch sorption experiments were carried out in 100 mL Erlenmeyer flasks, where 0.005–0.03 g of the $CoFe_2O_4$@PEI and 50 mL of the DB solutions (10–35 mg L^{-1}) were added following pH (2–8) adjustment (using diluted acid or base) and irradiated by ultrasonic irradiation (2–7 min). Then, the $CoFe_2O_4$@PEI was separated by an external magnetic field and the concentration of the DB in the solution after equilibrium adsorption was measured at 620 nm. The removal percentage of DB at equilibrium was calculated by:

$$R(\%) = \frac{(C_0 - C_e)}{C_0} \times 100 \quad (1)$$

where C_0 and C_e (mg L^{-1}) are the liquid-phase concentrations of DB at initial and equilibrium, respectively.

3. Results and discussion

3.1. Characterization of Co-Fe_2O_4@PEI

Fig. 2 represents the FTIR spectra of $CoFe_2O_4$, $CoFe_2O_4@SiO_2$, Co-$Fe_2O_4@SiO_2$-Cl, and $CoFe_2O_4@SiO_2$@PEI, respectively. The characteristic peak at 585 cm^{-1} is related to Fe–O stretching which is observed in four stages even after polymer coating samples and chemical modification. However, the intensity of the Fe–O peak reduced comparatively with further modification and approximate formation of shells that show the successful modification of $CoFe_2O_4$ nanoparticles. The characteristic peaks at 681 cm^{-1}, 1267 cm^{-1} and 1424 cm^{-1} are attributed to N–H, C–N and C–H bonds respectively, while the characteristic peaks at 2977, 2925, and 2856 cm^{-1} are related to C–H vibrations peaks of C–H in CH_2 groups. These characteristic absorptions denote that polyethyleneimine has been successfully grafted onto the silica surface. Fig. 3 shows

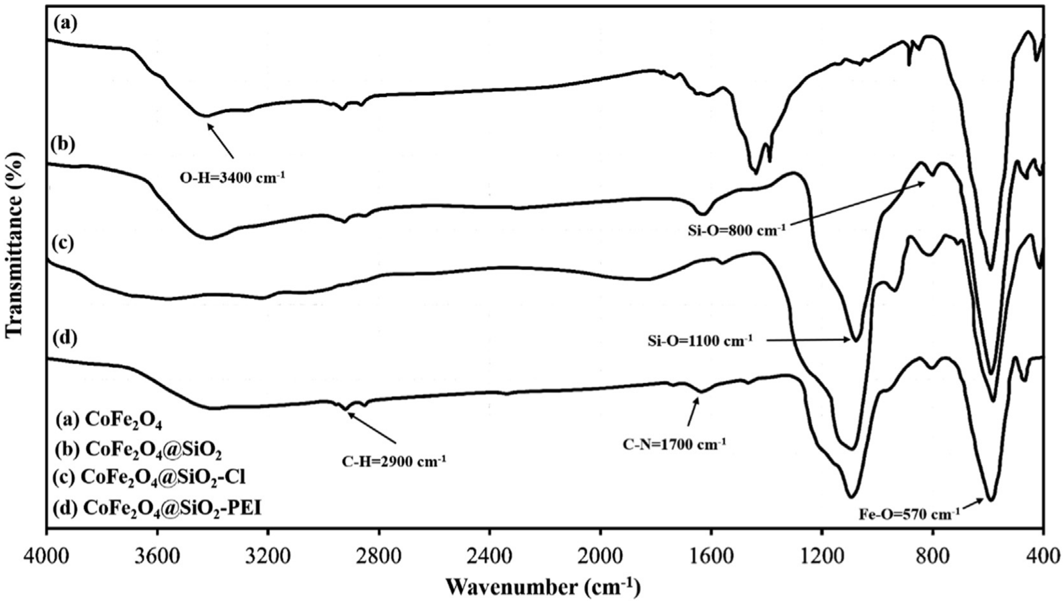

Fig. 2 FTIR spectra of $CoFe_2O_4$, $CoFe_2O_4@SiO_2$, $CoFe_2O_4@SiO_2$-Cl and $CoFe_2O_4@SiO_2$@PEI.

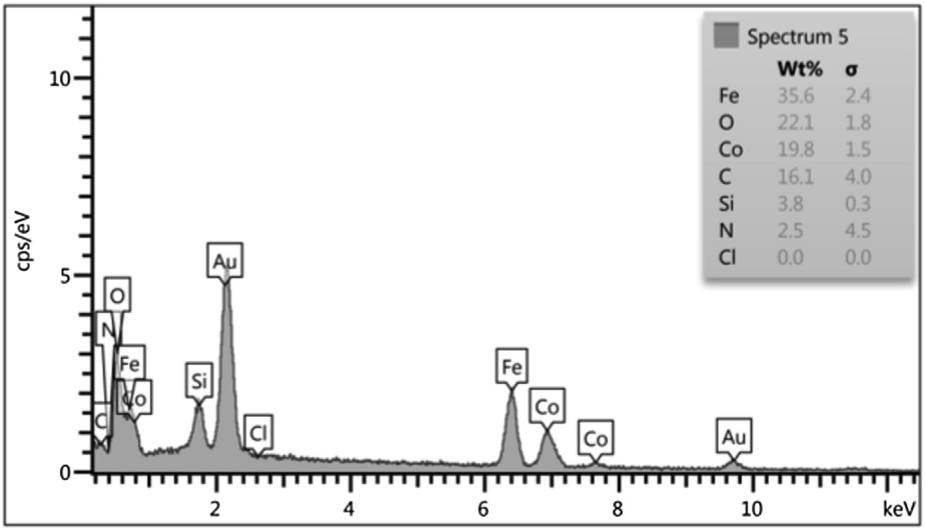

Fig. 3 EDX analysis of $CoFe_2O_4$@ PEI.

the EDX analysis of $CoFe_2O_4$@PEI which confirms the presence of the Fe, O, Co, C, N, and Si with an approximate mass ratio of 35.6, 22.1, 19.8, 16.1, 2.5, and 3.8% respectively. In should be pointed out that the presence of N and the absence of Cl proves that PEI was formed and 3-chloropropyl removed on the surface of $CoFe_2O_4$@SiO_2. Fig. 4 represents the XRD pattern of $CoFe_2O_4$@PEI in which diffraction peaks located at $2\theta = 30.09$, 35.44, 37.06, 43.06, 47.15, 53.45, 56.98, 62.59, 65.76, 70.95, 74.01, 75.01, and 78.97 could be well attributed to the (2 2 0), (3 1 1), (2 2 2), (4 0 0), (4 2 2), (5 1 1), (4 4 0), (5 3 1), (6 2 0), (5 3 3), (6 2 2), and (4 4 4). These are related to a cubic unit cell and approve the cubic spinel structure (JCPDS No. 00-022-1086). The expanded XRD lines indicate that the particles are in nano-size range and, according to Scherer Eq., are based on a distinguished peak of (3 1 1) plane: the calculated values of the size corresponding to $CoFe_2O_4$-NPs were 18.0 nm. Fig. 5 indicates the FESEM image of $CoFe_2O_4$@PEI which shows that the spherical shapes of prepared sorbent with a low degree of agglomeration that is corresponds to the magnetic properties of $CoFe_2O_4$@PEI. The structure of $CoFe_2O_4$@PEI was evaluated by TEM analysis (Fig. 6). TEM image shows that the SiO_2@PEI layer is anchored on the surface of $CoFe_2O_4$ nanoparticle successfully. The thickness of the SiO_2@PEI layer leads to a fast mass transfer of DB, which decreases removal time as well as enhances in the performance and applicability of the proposed sorbent. To investigate the magnetic properties of $CoFe_2O_4$, VSM was applied. As can be seen in Fig. 7, saturation magnetization is nearly constant at 60 emu g^{-1} that shows the strong magnetization property of $CoFe_2O_4$ nanoparticles.

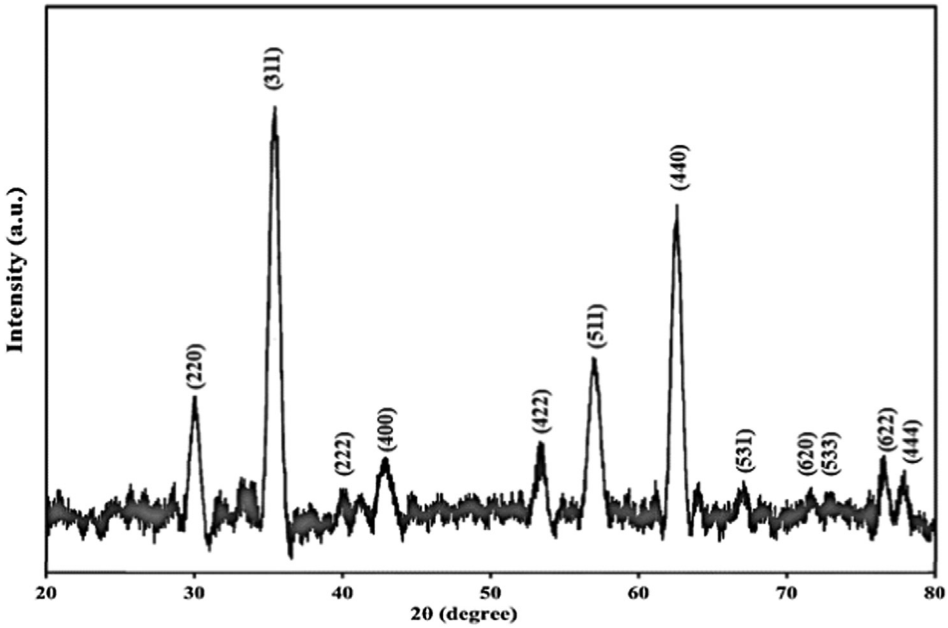

Fig. 4 XRD pattern of $CoFe_2O_4$@ PEI.

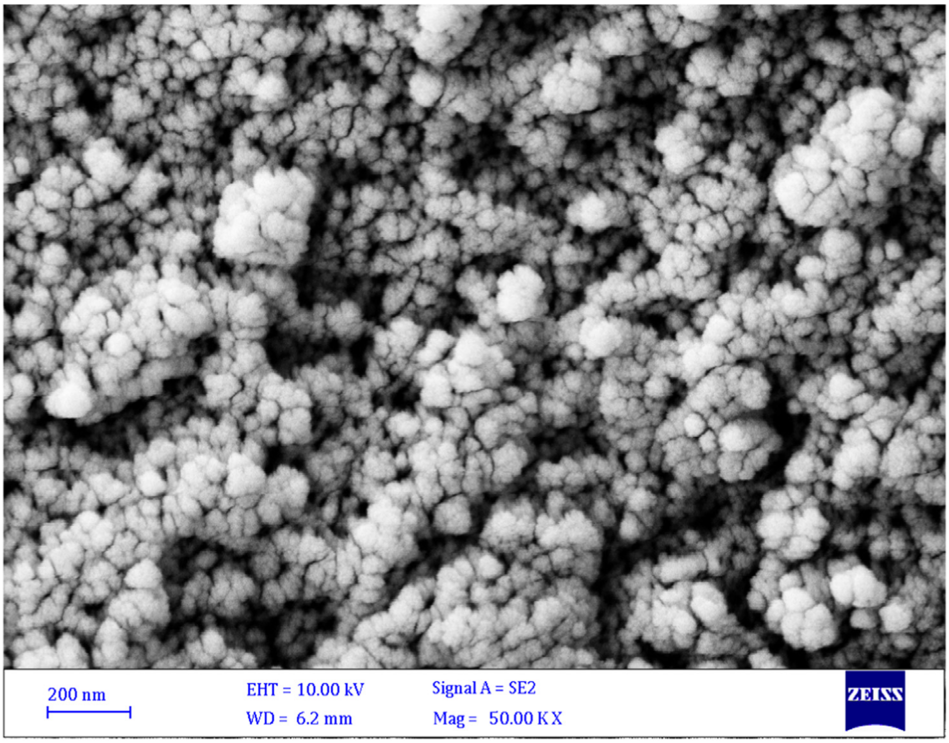

Fig. 5 FESEM image of $CoFe_2O_4$@ PEI.

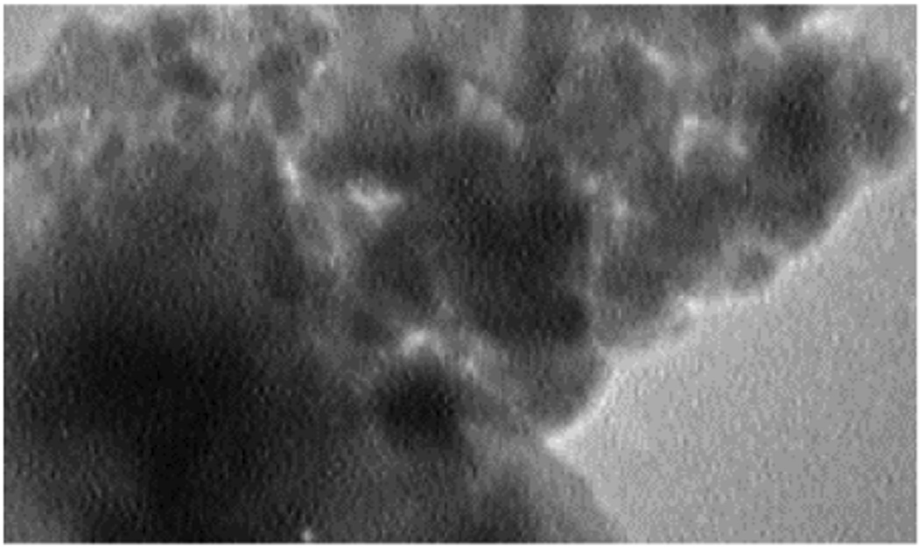

Fig. 6 TEM image of $CoFe_2O_4$@ PEI.

3.2. Optimization of effective parameters

The effect of four parameters on removal percentage including pH, sorbent mass, ultrasonic time and Disulfine blue concentration were evaluated individually. The solution pH is one of the most important parameters that can affect and change the ionic or neutrality state of DB and Fe_2O_4@PEI and has a noticeable role in the removal of SY. In this regard, for finding the optimum pH, the effect of pH solution was examined in the range of 2.0–8.0 (Fig. S1). The optimum extraction recovery was achieved at pH 5.0. This phenomenon is probably due to hydrogen bonding interactions between NH^+ groups of PEI and SO_3^- groups of DB at pH 5.0. At pH 5, N-H groups on the surface of Fe_2O_4@PEI get a positive charge and can interact thought hydrogen bond with SO_3^- of DB. At pH values lower than 5.0, the removal percentage was decrease that due to change in stability of $CoFe_2O_4$ @PEI. On the other hand, under strongly alkaline conditions, PEI cannot be protonated

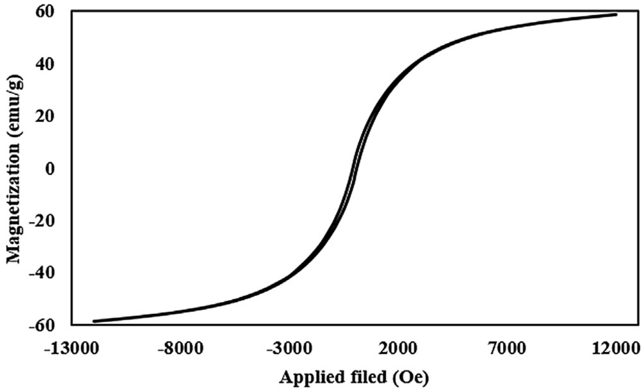

Fig. 7 VSM image of $CoFe_2O_4$@ PEI.

which decreases the electrostatic interaction for adsorption. Therefore, pH 5.0 was selected as optimum pH for the next experiments. Fig. S2 shows the effect of sorbent dosage on removal of DB was evaluated in the range of 0.005–0.03 g. As can be seen in Fig. S2, the maximum removal percentage was achieved at 0.015 g of $CoFe_2O_4$@PEI. An adequate amount of sorbent dosage can increase specific surface area and adsorption capacity which subsequently rise the removal percentage, while the inadequate amount of sorbent has the opposite effect and can decrease specific surface area and mass transfer and subsequently decrease removal percentage. Fig. S3 represents the effect of ultrasonic time in the range of 2.0–7.0 min. Results showed that maximum removal percentage was obtained at 5.0 min. Ultrasonic irradiation can enhance the contact surface between DB molecules and $CoFe_2O_4$@PEI and then increase the removal of SY molecules. The decrease of removal percentage at a time more than 5 min is probably due to desorption of DB molecules from $CoFe_2O_4$@PEI. Also, the effect of DB concentration was assessed in the concentration range of 10.0–35.0 mg L^{-1}. The effect of initial DB concentration on the removal percentage reveals that maximum removal was observed at 10.0 mg L^{-1} of DB concentrations that is due to a low ratio of solute concentrations to adsorbent sites while in high DB concentrations it has the opposite effect (Fig. S4). Fig. S5 shows the UV–Vis spectra of disulfine blue before and after removal at optimum conditions.

3.3. *Adsorption isotherms assessment for removal of DB by $CoFe_2O_4$@PEI*

The adsorption isotherm is an important aspect of adsorption study that shows the affinity, tendency as well as adsorption mechanism of analyte toward sorbent. Therefore, different isotherm models including Langmuir, Freundlich, Temkin, and Dubinin–Radushkevich were evaluated as listed in Table S1. According to Table S1, q_e shows the adsorbed DB at equilibrium, Q_m is the maximum adsorption capacity, C_e is the DB concentration in sample solution at equilibrium, K_L, R_L, K_F, 1/n, B_1, K_T, and K are the Langmuir, Freundlich, Temkin, and Dubinin–Radushkevich constants, respectively (Agarwal et al., 2016). Based on Fig. S6, Q_m for was achieved to be 110.0 mg g^{-1}. The R^2 for Langmuir model (0.9983) was higher than other models which confirms that the adsorption of DB onto $CoFe_2O_4$@PEI can be well described by Langmuir isotherm. The principle of Langmuir isotherm is based on the monolayer adsorption of DB molecules onto the homogenous surface of sorbent while the Freundlich model assumes the multilayer adsorption of DB molecules onto the heterogeneous surface of the sorbent. Considering the previous discussion on the effect of pH, it is speculated that the DB molecules are monolayer adsorbed on the surface of $CoFe_2O_4$@PEI mainly through hydrogen interactions. R_L is a separation factor that can take values between 0 and 1 which show desire (irreversible) and undesired (reversible) adsorption, respectively. The R_L for DB adsorption onto $CoFe_2O_4$@PEI was achieved to be 0.017–0.067 that is near to 0 and shows a desire (irreversible adsorption) process. 1/n shows the adsorption intensity. If n take values between 0 and 1 show that the adsorption process is favorable. B is the Temkin constant related to the heat of sorption. Dubinin–Radushkevich represents the physical and/or chemical nature of adsorption. If E values are between 8 and 16 KJ mol^{-1} chemical mechanism controlled the adsorption process while for E lower than 8 KJ mol^{-1}, the adsorption process occurs through a physical mechanism.

3.4. *Adsorption kinetic investigation for adsorption of SY by COFNP*

To examine the dynamics of the adsorption process in terms of the order of rate constant, different adsorption kinetics such as First-order-kinetic, Pseudo-second-order-kinetic, Intraparticle diffusion, and Elovich were studied. Based on Table S2, q_e and q_t are the adsorbed DB at equilibrium and time t, K_1, K_2, K_{diff}, C, β and α are the constants of models, respectively. According to Table S2, R2 value for the Pseudo-second-order-kinetic model (0.9972) was higher than other models which confirms that adsorption kinetic followed by Pseudo-second-order. Also, the theoretical $q_{e(cal)}$ value was close to the experimental $q_{e(exp)}$ value for Pseudo-second-order-kinetic model which implies that the second-order model is in good agreement with experimental data and can be used to favorably explain the DB adsorption on $CoFe_2O_4$@PEI.

3.5. *Reusability of $CoFe_2O_4$@PEI*

To investigate the practical aspect of prepared $CoFe_2O_4$@PEI, the reusability of the sorbent was examined. In this regard, different adsorption-desorption cycles of $CoFe_2O_4$@PEI were completed and results represented that the prepared $CoFe_2O_4$@PEI is applicable for at least five times (Fig. S7). Thus, the proposed $CoFe_2O_4$@PEI is a good candidate for practical application for the removal of DB from an aqueous solution.

3.6. *Comparison of the presented method*

The presented method was compared with some other reported methods and results are presented in Table S3. As can be seen from Table S3, the prepared sorbent has high adsorption capacity (110.0 mg g^{-1}) and also short extraction time (5.0 min). The prepared sorbent has a nano-diameter size which has extensive properties in terms of high chemical and physical stability, high contact surface area and also high adsorption capacity. The magnetic property of prepared sorbent eliminates the use of centrifuge, filtration and also precipitation methods for a gathering of the sorbent. In addition, the magnetic property of sorbent decreases removal time and also enhances repeatability of sorbent and also proposed method (Bagheri et al., 2016a; Savari et al., 2019; Wang et al., 2018).

4. Conclusion

In the present study, a novel nano-composite namely $CoFe_2O_4$@PEI was prepared and subsequently used as an adsorbent for ultrasonic-assisted removal of disulfine blue dye from aqueous solution. In this study was tried to introduce magnetic nanoparticles for the removal of disulfine blue from water samples. The magnetic property of sorbent accelerates the isolation of sorbent without using filtration, centrifuge and precipitation procedures. Also, it can decrease the removal time and also enhances the contact surface area and repeatability of the proposed method. It was observed that the combination of ultrasonic irradiation with $CoFe_2O_4$@PEI is an efficient, fast and applicable adsorption method for the removal of disulfine blue dye. The adsorption capacity of the applied adsorbent was found to be 110.0 mg g^{-1}. The influences of experimental parameters on the DB removal percentage were successfully investigated and the optimum conditions were obtained as follows: pH of 5.0, sorbent dosage of 0.015 g, ultrasonic time of 5.0 min and initial concentration of 10.0 mg L^{-1}. The isotherm models such as Langmuir, Freundlich, and Temkin were evaluated and it was shown that the equilibrium data were best described by the Langmuir model. Also, the process kinetics was successfully fitted to the pseudo-second-order kinetic model. Generally, routine synthesis approaches are faced with main drawbacks in terms of high consumption of organic, toxic and expensive sorbent, multi-step approaches that are time-consuming, low mass transfer and also low adsorption capacity. One of the main plans for future researches is using green and sustainable synthesis approaches for the fabrication of applicable sorbent for removal of hazardous materials from the environment especially water samples without using a hazardous, toxic, organic and expensive solvent. The other main plan is a synthesis and using hollow porous sorbent to increase the mass transfer and also adsorption capacity. The other plan is a synthesis of a selective sorbent like molecularly imprinted polymers for selective removal of one or many compounds from the environment especially complex matrixes. Also, we will try to combinate the molecularly imprinted polymers with excellent sorbents like metal-organic frameworks and also covalent organic frameworks to introduce a selective sorbents with high adsorption capacity.

Appendix A. Supplementary data

Supplementary data to this article can be found online at https://doi.org/10.1016/j.arabjc.2020.03.022.

References

Agarwal, S., Tyagi, I., Gupta, V.K., Bagheri, A.R., Ghaedi, M., Asfaram, A., Hajati, S., Bazrafshan, A.A., 2016. Rapid adsorption of ternary dye pollutants onto copper (I) oxide nanoparticle loaded on activated carbon: Experimental optimization via response surface methodology. J. Environ. Chem. Eng. 4 (2), 1769–1779.

An, F., Gao, B., 2007. Chelating adsorption properties of PEI/SiO2 for plumbum ion. J. Hazard. Mater. 145 (3), 495–500.

Ansari, S.M., Sinha, B.B., Phase, D., Sen, D., Sastry, P.U., Kolekar, Y.D., Ramana, C.V., 2019. Particle size, morphology, and chemical composition controlled CoFe2O4 nanoparticles with tunable magnetic properties via oleic acid based solvothermal synthesis for application in electronic devices. ACS Appl. Nano Mater. 2 (4), 1828–1843.

Arabi, M., Ghaedi, M., Ostovan, A., 2017. Water compatible molecularly imprinted nanoparticles as a restricted access material for extraction of hippuric acid, a biological indicator of toluene exposure, from human urine. Microchim. Acta 184 (3), 879–887.

Arabi, M., Ostovan, A., Bagheri, A.R., Guo, X., Li, J., Ma, J., Chen, L., 2020. Hydrophilic molecularly imprinted nanospheres for the extraction of rhodamine B followed by HPLC analysis: A green approach and hazardous waste elimination. Talanta. 120933.

Arabi, M., Ostovan, A., Ghaedi, M., Purkait, M.K., 2016. Novel strategy for synthesis of magnetic dummy molecularly imprinted nanoparticles based on functionalized silica as an efficient sorbent for the determination of acrylamide in potato chips: optimization by experimental design methodology. Talanta 154, 526–532.

Bagheri, A.R., Arabi, M., Ghaedi, M., Ostovan, A., Wang, X., Li, J., Chen, L., 2019a. Dummy molecularly imprinted polymers based on a green synthesis strategy for magnetic solid-phase extraction of acrylamide in food samples. Talanta 195, 390–400.

Bagheri, A.R., Arabi, M., Ghaedi, M., Ostovan, A., Wang, X., Li, J., Chen, L.J.T., 2019b. Dummy molecularly imprinted polymers based on a green synthesis strategy for magnetic solid-phase extraction of acrylamide in food samples. 195, 390–400.

Bagheri, A.R., Ghaedi, M., 2019. Synthesis of chitosan based molecularly imprinted polymer for pipette-tip solid phase extraction of Rhodamine B from chili powder samples. Int. J. Biol. Macromol. 139, 40–48.

Bagheri, A.R., Ghaedi, M., 2020a. Application of Cu-based metal-organic framework (Cu-BDC) as a sorbent for dispersive solid-phase extraction of gallic acid from orange juice samples using HPLC-UV method. Arabian J. Chem. 13, 5218–5228.

Bagheri, A.R., Ghaedi, M., 2020b. Green preparation of dual-template chitosan-based magnetic water-compatible molecularly imprinted biopolymer. Carbohydrate Polym. 116102.

Bagheri, A.R., Ghaedi, M., 2020c. Magnetic metal organic framework for pre-concentration of ampicillin from cow milk samples. J. Pharm. Anal.

Bagheri, A.R., Ghaedi, M., Asfaram, A., Bazrafshan, A.A., Jannesar, R.J.U.s., 2017. Comparative study on ultrasonic assisted adsorption of dyes from single system onto Fe3O4 magnetite nanoparticles loaded on activated carbon: experimental design methodology. 34, 294–304.

Bagheri, A.R., Ghaedi, M., Asfaram, A., Hajati, S., Ghaedi, A.M., Bazrafshan, A., Rahimi, M.R., 2016a. Modeling and optimization of simultaneous removal of ternary dyes onto copper sulfide nanoparticles loaded on activated carbon using second-derivative spectrophotometry. J. Taiwan Inst. Chem. Eng. 65, 212–224.

Bagheri, A.R., Ghaedi, M., Asfaram, A., Hajati, S., Ghaedi, A.M., Bazrafshan, A., Rahimi, M.R.J.J.o.t.T.I.o.C.E., 2016b. Modeling and optimization of simultaneous removal of ternary dyes onto copper sulfide nanoparticles loaded on activated carbon using second-derivative spectrophotometry. 65, pp. 212–224.

Bagheri, A.R., Ghaedi, M., Asfaram, A., Jannesar, R., Goudarzi, A.J. U.s., 2017. Design and construction of nanoscale material for ultrasonic assisted adsorption of dyes: application of derivative spectrophotometry and experimental design methodology. 35, 112–123.

Bidgoli, H., Mortazavi, Y., Khodadadi, A.A.J.J.o.h.m., 2019. A functionalized nano-structured cellulosic sorbent aerogel for oil spill cleanup: Synthesis and characterization. 366, 229–239.

Gholami, H., Arabi, M., Ghaedi, M., Ostovan, A., Bagheri, A.R., 2019a. Column packing elimination in matrix solid phase dispersion by using water compatible magnetic molecularly imprinted polymer for recognition of melamine from milk samples. J. Chromatogr. A 1594, 13–22.

Gholami, H., Ghaedi, M., Arabi, M., Ostovan, A., Bagheri, A.R., Mohamedian, H., 2019b. Application of molecularly imprinted biomembrane for advancement of matrix solid-phase dispersion for clean enrichment of parabens from powder sunscreen samples: optimization of chromatographic conditions and green approach. ACS Omega 4 (2), 3839–3849.

Gholami, H., Ghaedi, M., Ostovan, A., Arabi, M., Bagheri, A.R., 2019c. Preparation of hollow porous molecularly imprinted and aluminum (III) doped silica nanospheres for extraction of the drugs valsartan and losartan prior to their quantitation by HPLC. Microchim. Acta 186 (11), 702.

Guo, X., Li, J., Arabi, M., Wang, X., Wang, Y., Chen, L., 2020. Molecular imprinting-based surface-enhanced Raman scattering sensors. ACS Sensors.

Homem, N.C., Beluci, N.d.C.L., Amorim, S., Reis, R., Vieira, A.M.S., Vieira, M.F., Bergamasco, R., Amorim, M.T.P.J.A.S.S., 2019. Surface modification of a polyethersulfone microfiltration membrane with graphene oxide for reactive dyes removal.

Khani, R., Sobhani, S., Yari, T.J.M.J., 2019. Magnetic dispersive micro solid-phase extraction of trace Rhodamine B using iminopyridine immobilized on iron oxide as nanosorbent and optimization by Box–Behnken design. 146, 471–478.

Li, C., Yang, Q., Wang, X., Arabi, M., Peng, H., Li, J., Xiong, H., Chen, L., 2020. Facile approach to the synthesis of molecularly imprinted ratiometric fluorescence nanosensor for the visual detection of folic acid. Food Chem. 126575.

Maaz, K., Mumtaz, A., Hasanain, S.K., Ceylan, A., 2007. Synthesis and magnetic properties of cobalt ferrite (CoFe2O4) nanoparticles prepared by wet chemical route. J. Magn. Magn. Mater. 308 (2), 289–295.

Ostovan, A., Ghaedi, M., Arabi, M., 2018a. Fabrication of water-compatible superparamagnetic molecularly imprinted biopolymer for clean separation of baclofen from bio-fluid samples: a mild and green approach. Talanta 179, 760–768.

Ostovan, A., Ghaedi, M., Arabi, M., Yang, Q., Li, J., Chen, L., 2018b. Hydrophilic multitemplate molecularly imprinted biopolymers based on a green synthesis strategy for determination of B-family vitamins. ACS Appl. Mater. Interfaces 10 (4), 4140–4150.

Oussalah, A., Boukerroui, A., Aichour, A., Djellouli, B.J.I.j.o.b.m., 2019. Cationic and anionic dyes removal by low-cost hybrid alginate/natural bentonite composite beads: Adsorption and reusability studies. 124, 854–862.

Pastor-Belda, M., Viñas, P., Campillo, N., Hernández-Córdoba, M., 2017. Magnetic solid phase extraction with CoFe2O4/oleic acid nanoparticles coupled to gas chromatography-mass spectrometry for the determination of alkylphenols in baby foods. Food Chem. 221, 76–81.

Savari, A., Heidarizadeh, F., Pourreza, N., 2019. Synthesis and characterization of CoFe2O4@ SiO2@ NH-NH2-PCuW as an acidic nano catalyst for the synthesis of 1, 4-benzodiazepines and a powerful dye remover. Polyhedron 166, 233–247.

Stöber, W., Fink, A., Bohn, E., 1968. Controlled growth of monodisperse silica spheres in the micron size range. J. Colloid Interface Sci. 26 (1), 62–69.

Tanhaei, B., Ayati, A., Sillanpää, M.J.I.j.o.b.m., 2019. Magnetic xanthate modified chitosan as an emerging adsorbent for cationic azo dyes removal: Kinetic, thermodynamic and isothermal studies. 121, 1126–1134.

Uogintė, I., Lujanienė, G., Mažeika, K.J.J.o.h.m., 2019. Study of Cu (II), Co (II), Ni (II) and Pb (II) removal from aqueous solutions using magnetic Prussian blue nano-sorbent. 369, 226–235.

Wang, J., Liu, M., Chen, T., Chen, J., Ge, W., Fu, Z., Peng, R., Zhai, X., Lu, Y., 2018. Core-shelled mesoporous CoFe2O4–SiO2 material with good adsorption and high-temperature magnetic recycling capabilities. J. Phys. Chem. Solids 115, 300–306.

Wang, X., Yu, S., Wang, J., Yu, J., Arabi, M., Fu, L., Li, B., Li, J., Chen, L., 2020. Fluorescent nanosensor designing via hybrid of carbon dots and post-imprinted polymers for the detection of ovalbumin. Talanta 211. 120727.

Yang, G., Guo, Q., Yang, D., Peng, P., Li, J., 2019. Disperse ultrafine amorphous SiO2 nanoparticles synthesized via precipitation and calcination. Colloids Surf., A 568, 445–454.

Yang, Q., Li, C., Li, J., Arabi, M., Wang, X., Peng, H., Xiong, H., Choo, J., Chen, L., 2020a. Multi-emitting fluorescence sensor of MnO2-OPD-QDs for the multiplexed and visual detection of ascorbic acid and alkaline phosphatase. J. Mater. Chem. C.

Yang, Q., Li, C., Li, J., Wang, X., Arabi, M., Peng, H., Xiong, H., Chen, L., 2020b. Rational construction of a triple emission molecular imprinting sensor for accurate naked-eye readout of folic acid. Nanoscale.

Yang, Q., Wang, X., Peng, H., Arabi, M., Li, J., Xiong, H., Choo, J., Chen, L., 2020c. Ratiometric fluorescence and colorimetry dual-mode assay based on manganese dioxide nanosheets for visual detection of alkaline phosphatase activity. Sens. Actuators, B 302. 127176.

Zangeneh, H., Zinatizadeh, A.A., Zinadini, S., Feyzi, M., Bahnemann, D.W., 2019. Preparation and characterization of a novel photocatalytic self-cleaning PES nanofiltration membrane by embedding a visible-driven photocatalyst boron doped-TiO2SiO2/CoFe2O4 nanoparticles. Sep. Purif. Technol. 209, 764–775.

Zhang, M., Yang, J., Geng, X., Li, Y., Zhenxing, Z., Cui, S., Yang, J., 2019. Magnetic adsorbent based on mesoporous silica nanoparticles for magnetic solid phase extraction of pyrethroid pesticides in water samples. J. Chromatogr. A.

Zhong, Z., Jia, L., 2019. Room temperature preparation of water-soluble polydopamine-polyethyleneimine copolymer dots for selective detection of copper ions. Talanta 197, 584–591.

Zhou, Q., Zheng, Z., Xiao, J., Fan, H., 2016. Sensitive determination of As (III) and As (V) by magnetic solid phase extraction with Fe@polyethyleneimine in combination with hydride generation atomic fluorescence spectrometry. Talanta 156–157, 196–203.